Modeling and Simulation Study of Electrical Properties of Ge-on-Si Diodes with Nanometer-thin PureGaB Layer

L. Marković*[1], T. Knežević[1,2] and L.K. Nanver[2] and T. Suligoj[1]
[1]University of Zagreb, Faculty of Electrical Engineering and Computing, Micro and Nano Electronics Laboratory
[2]University of Twente, Faculty of Electrical Engineering Mathematics & Computer Science
*lovro.markovic2@fer.hr

***Abstract* - Deposition of a nanometer-thin layer-stack of pure gallium and boron (PureGaB) on arsenic (As)-doped epitaxial germanium (Ge) forms a shallow-junction photodiode, reported to have almost ideal *I-V* characteristics, low saturation current densities, and high responsivity down to 255 nm wavelengths. In this work, different physical mechanisms that could explain the high anode Gummel number in PureGaB-Ge-on-Si diode have been examined. A model for point-defect-mediated diffusion of B and Ga in Ge has been developed. Formation of a shallow pn junction has been modeled using 1D process simulations of B and/or Ga drive-in from the PureGaB layer. B diffusion resulted in junction depths less than a nanometer deep, while Ga formed a highly doped p^+ regions with peak concentrations $>10^{20}$ cm^{-3} and junction depths from 31 nm to 123 nm, depending on the applied sets of diffusion parameter. Both approaches have been used to fit the *I-V* characteristics of a fabricated PureGaB Ge-on-Si diode: B-only diffusion model with negative interface charge concentration of 1.9 10^{13} cm^{-2} for suppression of electron injection and Ga diffusion model, self-sufficient for the explanation of low electron current densities. Both proposed models give possibilities to obtain a Gummel number of $\approx 2\times10^{14}$ s/cm^4, matching the value extracted from *I-V* characteristics of a fabricated device.**

Keywords – PureGaB, Ge-on-Si, germanium, detector, infrared, gallium, boron, diffusion, process simulations, anode Gummel number, interface charge layer

I. Introduction

For almost half a century, Ge role in commercial-scale electronics has been minimal due to the lack of stable natural oxide. However, in terms of infra-red (IR) detection, it dominates over existing Si technology due to a narrower bandgap and higher carrier mobilities [1,2]. Even though narrow-bandgap III-V materials are also commercially available, their fabrication is expensive and less suitable for mass production due to the incompatibility with standard CMOS processes. About two decades ago, epitaxial growth of thin Ge films on top of the Si wafers arose as an idea for monolithic integration of a narrow bandgap material with CMOS technology. Methods for epitaxial growth of Ge-on-Si have been developed and high-quality crystalline (c-Ge) layers on Si wafer have been reported [1,3].

Deposition of a few-nanometers-thick layer of amorphous boron (PureB) on top of an n-Si substrate has been previously reported as a novel fabrication technique for formation of an ultra-shallow junction photodiode demonstrating high Gummel number i.e., with saturation current densities expected for a deep-junction Si diode. A similar approach for formation of a shallowly-doped p^+ region in n-doped Ge-on-Si has been reported by *Sammak et al.* [4]. The method consists of the deposition of a Ga wetting layer followed by a pure B deposition to form a p-type region on epitaxially-grown Ge-islands. In these "PureGaB" diodes, the nanometer-thin layer of PureGaB also serves as a material barrier, separating the Ge from an Al metallization. The *I-V* characteristics of Al-on-Ge-on-Si Schottky diode without PureGaB and Al-PureGaB-Ge-on-Si diode are both shown in Fig. 1(a). Low values of reverse current ($<10^{-14}$ A/µm^2), ideality factor close to unity ($n \leq 1.1$), low contact resistance, and high responsivity down to 255 nm wavelength has been demonstrated [3]. The latter requires high sensitivity within a few nanometers of the Ge surface. In PureB Si diodes this is achieved due to the damage-free ultrashallow p-type regions with gradients that create unidirectional electric fields without surface roll-off, thus efficiently suppressing the electron injection [5]. It is plausible that a similar mechanism is responsible for the PureGaB optoelelctronic behavior, making this device an ideal candidate for a CMOS-compatible broadband photodetector.

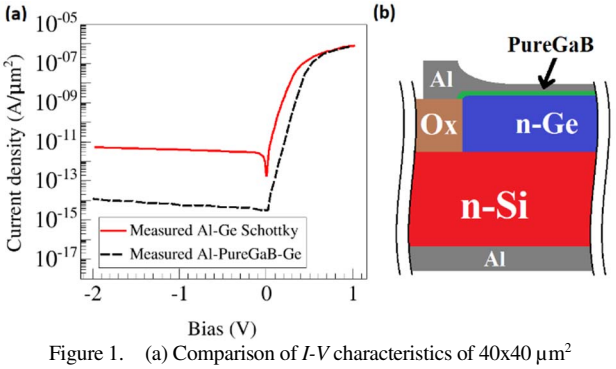

Figure 1. (a) Comparison of *I-V* characteristics of 40x40 µm^2 Al-Ge-on-Si Schottky diode and the equivalent-geometry diode with the addition of a PureGaB layer (targeted thickness 3 nm) between Ge and top-metallization [1]. Respective PureGaB *I-V* characteristics has been given for reference in all following figures depicting simulated *I-Vs*. (b) Simulated diode structure. Schematic does not correspond to the actual proportions of the diode.

The purpose of this work is to examine the degree of B/Ga diffusion that could be expected in the experimental

This work has been fully supported by Croatian Science Foundation under the project IP-2018-01-5296.

PureGaB diodes and the influence that this would have on the anode Gummel number and the junction depth. Firstly, we have performed process modeling and simulations of diffusion of B, while neglecting possible diffusion of Ga atoms. Additional physical phenomena – PureGaB bulk material properties, formation of a Schottky barrier on the anode contact and the fixed charge at PureGaB/Ge interface have been modeled to achieve a proper fit with measured PureGaB *I-V* characteristics. Secondly, a Ga diffusion model, based on the parameters taken from the literature, has been developed and utilized for process simulations of Ga diffusion into Ge. Finally, saturation currents and Gummel numbers of both B-diffusion and Ga-diffusion based diode models have been compared with the respective values extracted from the fabricated device.

II. Model and Parameters

The analyzed PureGaB Ge-on-Si diodes are fabricated on a n-type 2-5 Ω-cm Si (100) wafers. In particular, we focus on a diodes of dimensions 40×40 μm^2, as defined by an opening in a 1-μm thick surface SiO_2. Selective epitaxial growth of c-Ge within the oxide windows forms Ge-islands, about 1 μm thick. The Ge is in-situ arsenic doped with concentration of $\approx 10^{16}$ cm^{-3}. This is followed by the deposition of PureGa at 400 °C. Subsequent exposure to B_2H_6 at 700 °C for 30 min forms a thin capping layer of amorphous B. The targeted B thickness was 3 nm but due to loading effects it may be as thick as ~ 11 nm. Al metallization is sputtered and patterned to directly contact the PureGaB layer [1,3].

A TCAD model of a basic Ge-on-Si heterostructure has been previously developed [6]. Further diffusion simulations, after predeposition of Ga and amorphous B, have been performed using Sentaurus Process simulation software, following reported process parameters and fabrication steps [1]. Electrical characterization of the device model has been performed using Sentaurus Device.

A. Device parameters

The basic analyzed structure is shown in Fig. 1 (b). The bottom silicon layer with uniform phosphorus doping of $2 \cdot 10^{15}$ cm^{-3} was used as a substrate, which is equivalent to the 500-μm-thick Si wafer in a fabricated Ge-on-Si diode [1]. The modeled structure was 60-μm wide in total, while Si substrate thickness was varied to account for the spatial distribution of a cathode current over the large-area bottom contact. Centered on top of the Si substrate, a 1 μm thick and 40 μm wide Ge island was positioned between two SiO_2 regions, each 10 μm wide. The Ge layer was uniformly As-doped, with concentration of 10^{16} cm^{-3}. Such a 2D structure represents a vertical cross section of a real 40×40 μm^2 Ge-on-Si diode [1]. Since the measured 40×40 μm^2 diodes show only minor impact of the perimeter [1], bulk material properties, used for 1D simulations, are assumingly dominating the overall current. Therefore, process simulations in 1D have been carried out using a stacked structure of, bottom-up: Si, Ge, PureGaB and Al layers.

Material properties of the PureGaB layer, separating Ge-region and Al top-contact, has been defined according to the published references [7,8], and the B-thickness is set to 11 nm. A limited set of material and electrical characterization experiments on PureGaB properties have been performed so far. Measurements of sheet resistance of PureGaB layer deposited on the Si surface at 400 °C show no significant difference between sheet resistance of PureB and PureGaB [7]. Deposition at 700 °C in both cases results in reduction of sheet resistance which could be explained by B and/or Ga diffusion into silicon, thus forming a bulk-Si-doped p$^+$ region with higher mobilities and carrier concentrations than in the case of lateral current conduction along the Si surface with the low-temperature PureGaB/PureB layers only. The experimental span for electron and hole mobilities in PureB layer is between 10^{-3} cm^2/Vs and 10 cm^2/Vs and for concentration of free holes between 10^{17} and 10^{19} cm^{-3} [8]. Based on similar sheet resistances, free hole concentration in PureGaB model has been defined as in PureB – 2×10^{18} cm^{-3}. Carrier mobilities, on the other hand, can be considered insignificant in terms of *I-V* modeling, as the thickness of PureGaB is negligible compared to the thickness of the whole device. However, in this work we have used PureGa and PureB layers as a diffusion source of B and Ga atoms into the Ge island. In case of B, whole 11 nm-thick PureGaB layer has been used as a source for diffusion. In case of Ga, a predeposited layer thickness has been varied from a monoatomic layer to one of 1 nm thickness. Furthermore, the total dose of a Ga monolayer has been varied from 5×10^{12} cm^{-2} to 6.3×10^{14} cm^{-2}, the latter corresponding to the maximum available bonding sites on (100) Ge surface.

TABLE I. Boron and Gallium Diffusion Paramters

Parameter	Impurity		
	B	***Ga-shallow***	***Ga-deep***
D_0 (cm^2/s)	98500	8	34
E_a (eV)	4.65	3.21	3.1
V (cm^{-3}), 700 °C	$1.00 \cdot 10^{12}$		
I (cm^{-3}), 700 °C	$4.75 \cdot 10^{10}$		
SS (cm^{-3}), 700 °C	$2 \cdot 10^{18}$	$5 \cdot 10^{20}$	

Shockley-Read-Hall recombination in Ge was simulated using the doping-dependent lifetime model. Maximum carrier lifetimes for doping concentrations up to 10^{16} cm^{-3} are $\tau_e = 10^{-3}$ s and $\tau_h = 10^{-4}$ s [9, 10] with reduction of an order of magnitude per decade of dopant concentration [11]. *Phillips unified mobility model* [12] and *Fermi-Dirac* statistics for carrier distribution were used. Bandgap narrowing in a highly-doped degenerate semiconductor was modeled using Ge-specific parameters, obtained by *Jain* and *Roulston* [13]. Thermionic emission (TE) was used to model carrier transport across the heterojunction interfaces. Tunneling effects were disregarded in the entire device.

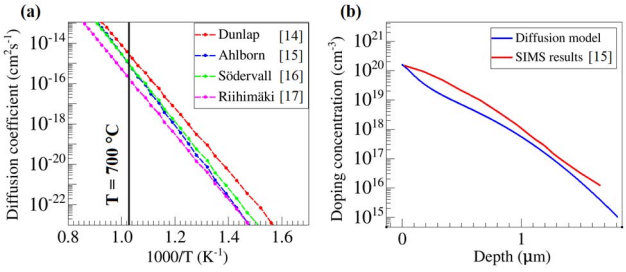

Figure 2. (a) Temperature dependence of Ga diffusion coefficients in Ge lattice extracted from different experiments. (b) Comparison of diffusion doping profile obtained in [15], with our model of vacancy-mediated diffusion, using the same process parameters (T = 713 °C, t = 5.78 10^5 s).

B. *Diffusion parameters*

The diffusivity of impurities in the crystal lattice is generally given by the Arrhenius law:

$$D = D_0 \exp\left(\frac{-E_a}{kT}\right), \quad (1)$$

where D_0 is a constant of the material and E_a activation energy (enthalpy) for the diffusion [14]. Diffusion parameters for B and Ga in Ge lattice are given in Table 1. Only a few experiments obtaining diffusion parameters for Ga in Ge have been reported, most of which are shown in Fig. 2 (a) [14-18].

Even though satisfactory for most purposes, the Arrhenius model assumes constant diffusivity in the crystal lattice, neglecting field-enhancement of the process and/or impurity-defect pairing. Impurity diffusion in Ge lattice is driven by point-defect self-diffusion and for most of the dopants, the process is vacancy mediated. B diffusion in Ge is slow as it requires non-dominant B-interstitial pairing. In contrast, Ga atoms in Ge lattice form Ga-vacancy pairs, diffusing at a rate similar to vacancy self-diffusion. Even though diffusing more efficiently than B, Ga migration in the lattice is slower than of the most n-type dopants in Ge, enabling formation of the shallow p-regions [16-21].

Correction of the basic Arrhenius diffusion model is given by Dunham and Wu, in the point-defect based equation for the approximation of diffusion activation enthalpy [22]:

$$E_a = E_V^f + E_V^m + \frac{E_{AV2} + E_{AV3}}{2}, \quad (2)$$

where E_V^f and E_V^m stand for the formation and migration enthalpies of a single isolated vacancy and E_{AV2} and E_{AV3} for binding energy with second and third vacancy, nearest to the impurity atom. The binding energy of a Ga atom with a single vacancy and GaV complex migration energy are calculated using charged-pair diffusion model [23]. Considering vacancy-mediated nature of the process and parameters from [18], process simulations result in the formation of significantly shallower pn junction, compared to those using older parameter sets. Furthermore, the model generates Ga deep-diffused tails which reduce effective n-type doping in the bulk Ge. To evaluate charged-pair Ga diffusion model from [18] and [23], the comparison of simulated doping profile and doping profile taken from [15] is shown in Fig. 2(b).

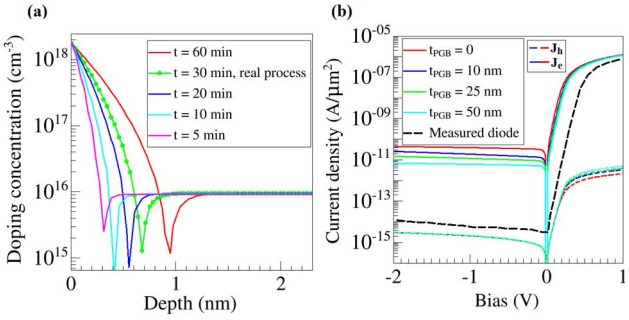

Figure 3. (a) B doping profile after drive-in into Ge at T = 700 °C. Simulation is performed using interstitial-mediated diffusion model. (b) Electron and hole current components of the diode with boron-diffused p-side for different thicknesses of overlaying p-doped PureGaB layer. Curves correspond to the diode after 30 minutes diffusion.

Simulations of B and Ga diffusion has been performed using interstitial-driven and vacancy-driven charged-pair model, respectively. Default values for intrinsic point-defect densities (V, I) in Ge have been used (see Table 1.) [24]. Solid solubility (SS) of Ga in Ge is the highest among all Ge dopants [21]. At 700 °C, which is a temperature of PureB deposition, thus being the highest temperature in the process – Ga solid solubility is more than two orders of magnitude higher than solubility of B. Solid solubility of B in Ge is $\approx 5\times10^{18}$ cm^{-3} at 850 °C [25, 26]. On the other hand, Ga solid solubility is 5×10^{20} cm^{-3} at 700 °C [21] or up to 1% of the mass fraction [27].

III. Results and Disscussion

Two different approaches for modeling of the PureGaB-Ge-on-Si diode were examined and compared.

Firstly, process simulations were performed by modeling diffusion of B from the PureGaB layer to underlying Ge substrate, while neglecting the Ga diffusion. This model was based on the assumption that Ga serves exclusively as a wetting layer for further deposition of PureB [8] and does not interact with bulk Ge. Therefore, the high anode Gummel number is attributed to either B-doped p^+ layer, electrostatic material properties of the PureGaB or the formation of a hole accumulation layer at the PureGaB-Ge interface due to the presence of negatively charged interface states. Similarly, the interface hole layer was already introduced and analyzed in the case of the PureB-Si interface [8, 28].

Secondly, the diffusion of Ga from the wetting layer into the underlying Ge has been examined. Ga diffusion has been simulated using process parameters discussed in Section II. The impact of the limited dose of Ga atoms in predeposited wetting layer and possible existence of charged interface states on *I-V* characteristics has been modeled.

A. *Boron-dominated diffusion model*

Process simulations of B diffusion from PureGaB into Ge are shown in Fig. 3(a). The 11-nm-thick PureGaB acted as a diffusion source with concentration of B atoms, $N_B = 10^{20}$ cm^{-3}, which is above the maximum solid solubility of B in Ge. After 30 minutes drive-in at 700 °C, corresponding to the real fabrication process in [1], the diffusion of B into Ge has been almost negligible. The p-n junction has formed at a depth of less than a nanometer. Furthermore, the maximum impurity concentration at the p-side was limited by the B solid solubility and have reached almost 2×10^{18} cm^{-3}. Due to the very shallow acceptor doping profile, electron injection from the bulk to the top electrode is dominating the total current. Considering that surface roughness could already exceed a nanometer, B diffusion in real devices could be essentially neglected. However, overlaying PureGaB, acting as a p-type semiconductor, gradually reduces the injection current with increase in thickness, as shown in Fig. 3(b). This is still not enough to explain the low forward and reverse currents measured in PureGaB Ge-on-Si diodes.

Another effect that could be used for fitting of the PureGaB diode *I-V* characteristics would be the formation of a Schottky barrier on the top contact, as shown in Fig. 4(a). The Schottky barrier height needed to suppress the electron current sufficiently would be $\Phi_B = 0.8$ eV.

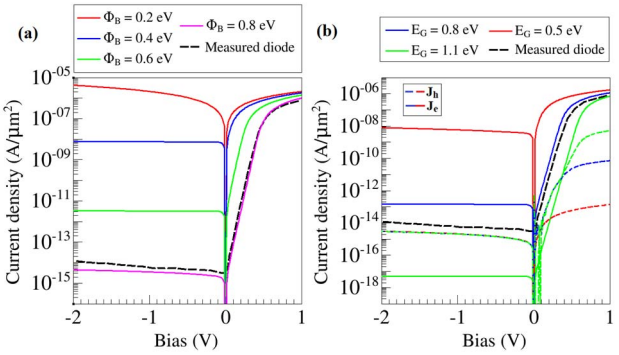

Figure 4. (a) Total current of a diode with boron-diffused p-side for different Schottky barrier heights at the anode. For purpose of this simulation, eventual discontinuity in the conduction band on the PureGaB-Ge interface has been neglected. Therefore, bandgap of PureGaB matches the bandgap of Ge, E_G = 0.66 eV. (b) Electron and hole current components of a diode with boron-diffused p-side for varying bandgap of the PureGaB layer. Ohmic boundary conditions have been applied. Curves correspond to the diode after 30 minutes diffusion.

However, such a barrier is much higher than any theoretical or experimental value. According to Schottky-Mott rule, based on the difference in Al workfunction and Ge electron affinity, the theoretical barrier height between Al and Ge is $\Phi_B \approx 0.08$ eV [6]. In addition, different authors report measured barriers in range 0.3 - 0.7 eV, with lower values generally extracted from *C-V* measurements and higher from *I-V* characteristics of diodes with a presumably defective Al/Ge interface – causing high contact resistances and poor ideality factor due to the interface oxide formation. [6, 29, 30]. Therefore, the formation of a top-contact rectifying barrier of Φ_B = 0.8 eV is unlikely.

Additional simulations were run by varying the bandgap of the PureGaB layer, assuming that the PureGaB layer can be modeled as a semiconductor. Although high atomic ratios of the conductor (Ga) in the Ga-B alloy might imply more metal-like properties, the measurements of the sheet resistance of PureGaB on a Si substrate show that the difference between the conductivity of PureB and PureGaB is within the statistical error [7]. Hence, the assumption of semiconducting nature of PureGaB could be considered reasonable. Therefore, we can further assume the possibility of potential barriers formed in the conduction band due to energy band mismatch between Ge and PureGaB. Experiments have shown that the PureB layer acts as a p-type semiconductor with a bandgap in range from

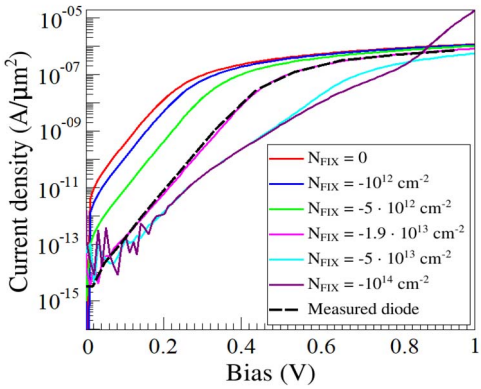

Figure 5. Total current of a diode with boron-diffused p-side for different concentrations of negative fixed charge at PureGaB/Ge interface. Curves correspond to the diode after 30 minutes diffusion.

0.55 eV to 0.8 eV [8]. Examining the effect of PureGaB's bandgap on *I-V* characteristics, only the values higher than maximum reported bandgap of 0.8 eV could explain a suppressed forward current, as shown in Fig. 4(b).

The best *I-V* fit using a boron-only diffusion model was achieved by introducing a negative fixed charge at the PureGaB-Ge interface forming a narrow layer of free holes. The layer acts as p^+ delta doping, which represents an energy barrier for the electrons. The modeled diode with a PureGaB-Ge interface charge density of 1.9×10^{13} cm^{-2} fits well with the measurements, as shown in Fig. 5.

B. Gallium-dominated diffusion model

The diffusion of Ga into the Ge island was simulated using models and parameters discussed in the Section II. Different values of the diffusion coefficients taken from the literature (see Table 1) result in significantly different doping profiles. Therefore, process simulations were performed using all four sets of Ga diffusion parameters shown in Fig. 2(a). A thin wetting layer of PureGa was defined as a limited source for Ga diffusion. Diffusion has been modeled for different doses of Ga atoms in the wetting layer. Based on the DFT study on surface bonding sites in (100) Si, which also has an FCC crystal structure [31], density of the surface states at (100) c-Ge surface has been calculated and equals 0.063 Å^{-2}. Therefore, sheet concentration (dose) of Ga atoms in a monoatomic wetting layer deposited on Ge is 6.3×10^{14} cm^{-2}, assuming all available surface states had been occupied. Furthermore, initial dose of 5×10^{12} cm^{-2} corresponds to surface state occupation less than 1%, while maximum simulated dose of 5.1×10^{15} cm^{-2} corresponds to a 1 nm-thick Ga crystalline layer. Different doping profiles after 30 min drive-in at 700 °C and corresponding *I-V* characteristics are shown in

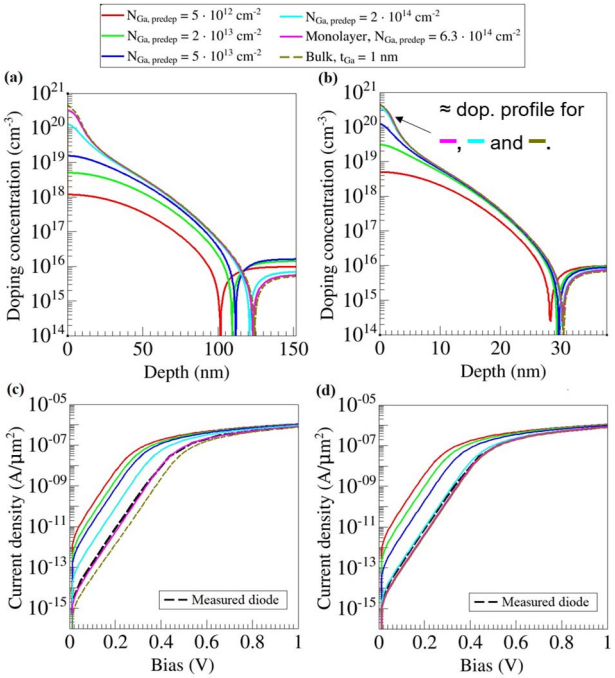

Figure 6. Ga doping profiles and respective I-V characteristics after drive-in into Ge at T = 700 °C and t = 30 min for different predeposited Ga doses. Simulation is performed using vacancy-mediated diffusion model using parameters from: *Dunlap et al.* – the deepest junction [(a) and (c)], and *Riihimäki et al.* – the shallowest junction [(b) and (d)].

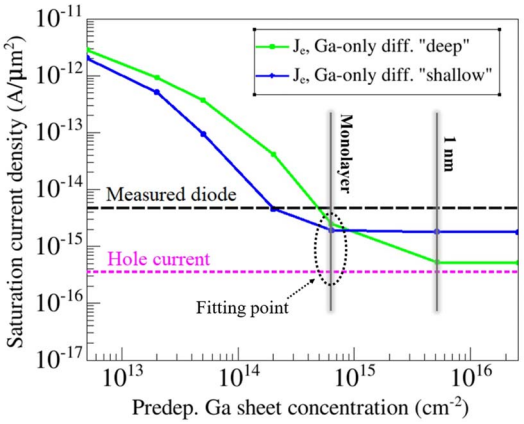

Figure 7. Comparison of electron and hole saturation currents for Ga-diffused p-side in respect to predeposited Ga dose. Values of predeposited sheet concentration corresponding to Ga monolayer and a 1 nm-thick layer of predeposited Ga are specially marked. Saturation current of the fabricated PureGaB diode is given for reference.

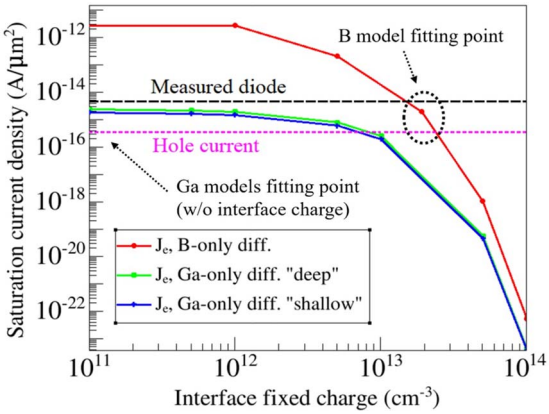

Figure 9. Comparison of electron and hole saturation currents for B and Ga-diffused p-side in respect to interface negative fixed charge concentration. Ga-diffused p-side correspond to predeposited Ga-monolayer, as shown on Fig. 6. Saturation current of the fabricated PureGaB diode is given for reference.

Fig. 6. The shallowest doping profile was obtained using parameters from the most recent work [18], while the deepest was obtained using parameters from pioneering work in the field [14]. Resulting metallurgical junction depths are 31 nm and 123 nm, respectively. The "deep" model by *Dunlap* results in deeper junctions, but also in a lower peak concentration, resulting in a higher current, as shown in Fig. 6(b) and (d). However, for doses exceeding 10^{15} cm^{-2}, both models reach peak acceptor concentration of 4×10^{20} cm^{-3} and a "deep" model results with lower saturation current densities. Further increase in predeposited dose does not impact the electrical characteristics of the device, as shown of Fig. 7. Diffusion from Ga monolayer has been taken as a referent model in further analysis as it matches the current of a fabricated device, in cases of both diffusion parameter sets. Simultaneous diffusion of B atoms from the PureGaB has been simulated, but due to the slow diffusion and the low peak concentration, B doping is negligible.

The introduction of a negative interface charge at the PureGaB/Ge interface further reduces the electronic component of the current. For concentration of interface charge above 10^{13} cm^{-2}, hole current dominates the overall current. Further increase in the interface charge concentration reduces the electron current, but the hole component remains unaffected, as shown in Fig. 8.

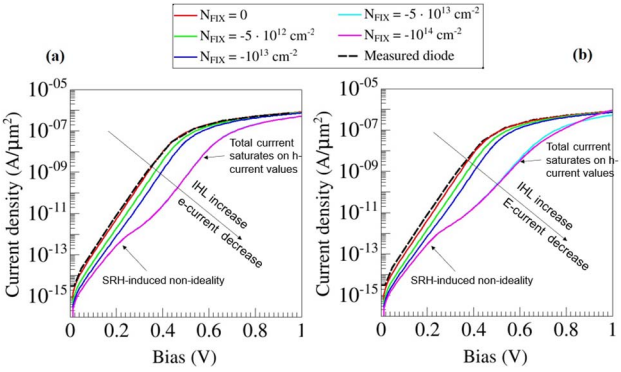

Figure 8. Total current of a diode with gallium-diffused p-side for different concentrations on negative fixed charge on PureGaB/Ge interface. P-side is formed after drive-in from predeposited Ga monolayer, as shown on Fig. 6. (a) Deep-diffused junction with pararameters taken from [14]. (b) Shallow-diffused junction with parameters taken from [18].

C. *Saturation current and Gummel number comparison for B-only and Ga diffusion models*

Both proposed technology models, based on either B-only or Ga diffusion, could explain the formation of a shallow pn junction with high Gummel number and low saturation current densities. In the case of B-diffused model, interface hole layer has stronger impact on total current, as it reduces the dominant electron component. Introduction of an interface charge layer is responsible for additional hole accumulation at the top interface, and is necessary for the explanation of the low saturation current density. In the case of the Ga-diffused model, the electron current component is already reduced and comparable to the hole component and the total current is mostly determined by the dopants in diffused p$^+$ region (Fig. 9).

The Gummel number extracted from the *I-V* characteristics accounts for all conduction mechanisms in the device. The ideal diode current can be written as:

$$I = \frac{q{n_i}^2}{G}\iint\left(e^{\frac{-V}{V_T}}-1\right)dxdy. \qquad (3)$$

Using (3), the anode Gummel number is:

$$G = \frac{q{n_i}^2}{J_S}, \qquad (4)$$

where J_S is the electron saturation current density, which can be extracted from current in forward bias. Anode Gummel numbers of B-diffused and Ga-diffused device models are given in Fig. 10. The Gummel number of a fabricated PureGaB diode has been extracted from *I-V* measurements and equals 1.3×10^{14} s/cm^4. In real devices, extraction of the anode Gummel number is possible only for devices where the electron current is dominant, which is confirmed by simulations in case of both fitted models. Significant increase occurs for sheet concentrations of interface charge above 2×10^{13} cm^{-2}, but in this region hole current becomes dominant (see Fig. 9). In the case when Boltzmann statistics is used for calculation, the increase of the anode Gummel number is proportional to the additional charge on p-side of the diode. However, in degenerate

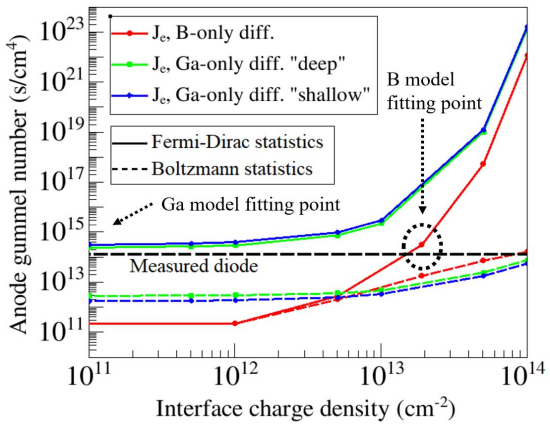

Figure 10. Comparison of anode Gummel numbers extracted from simulated electron currents in forward bias for B and Ga-diffused anode and different carrier distribution simulation models. Ga-diffused p-side correspond to predeposited Ga-monolayer, as shown in Fig. 6. Gummel number of the fabricated PureGaB diode has been extracted from forward-bias current and given for reference.

semiconductors with highly-doped regions, more accurate Fermi-Dirac statistics has to be employed and a sharp increase in anode Gummel number with respect to the increase of total charge can be observed in Fig. 10.

IV. Conclusion

The diffusion of dopants from the deposited PureGaB layer into the underlying Ge could result in different profiles depending on dominating dopant species.

If diffusion is dominated by B, process simulations result in junctions shallower than 1 nm with peak acceptor concentrations under 2×10^{18} cm^{-3}. However, if the PureGaB is a p-type semiconductor, it could act as the p-side of a PureGaB/n-Ge heterojunction, but this on its own cannot explain of high extracted anode Gummel number. Introduction of an interface hole layer is necessary to suppress the electron injection from the substrate.

If diffusion is dominated by Ga, drive-in from predeposited monoatomic wetting layer results in formation of a highly-doped p^+ side. The resulting deeper junctions, between 31 and 123 nm – depending on the diffusion model, are sufficient to suppress the electron injection.

With both proposed models it is possible to obtain a high Gummel number by using various contributions of dominant mechanisms, to match the values extracted from *I-V* characteristics of the fabricated device. An experimental determination of the junction depth would be needed to verify which mechanisms are in fact playing a role in the formation of the PureGaB anode region.

References

[1] A. Sammak, L. Qi, W. de Boer and L. Nanver, "PureGaB p+n Ge diodes grown in large windows to Si with a sub-300nm transition region", Solid-State Electron., vol. 74, pp. 126-133, 2012.

[2] J. Michel, J. Liu and L. Kimerling, "High-performance Ge-on-Si photodetectors", Nat. Photonics, vol. 4, no. 8, pp. 527-534, 2010. Quantum Electron., vol. 20, no. 6, pp. 306–316, Nov./Dec. 2014.

[3] T. Knežević, M. Krakers, L. K. Nanver, "Broadband PureGaB Ge-on-Si photodiodes responsive in the ultraviolet to near-infrared range," Proc. SPIE 11276, Opt. Compon. and Mater. XVII, 2020.

[4] A. Sammak, M. Aminian, Lin Qi, W. B. de Boer, E. Charbon and L. K. Nanver, "A CMOS compatible Ge-on-Si APD operating in proportional and Geiger modes at infrared wavelengths," Int. Electron Devices Meeting, pp. 8.5.1-8.5.4, 2011.

[5] L. Shi, S. Nihtianov, L. Haspeslagh, F. Scholze, A. Gottwald and L. K. Nanver, "Surface-Charge-Collection-Enhanced High-Sensitivity High-Stability Silicon Photodiodes for DUV and VUV Spectral Ranges," IEEE Trans. Electron Devices, vol. 59, no. 11, pp. 2888-2894, 2012.

[6] L. Marković, T. Knežević and T. Suligoj, "Modeling of Electrical Properties of Al-on-Ge-on-Si Schottky Barrier Diode," 2020 43rd Int. Conv. Inf., Commun. and Electron. Technol. (MIPRO), pp. 28-33, 2020.

[7] L. Qi, "Interface Properties of Group-III-Element Deposited-Layers Integrated in High-Sensitivity Si Photodiodes," PhD thesis, TU Delft, 2016.

[8] T. Knežević, " Physical charateristics and applications of nanometer thin boron-on-silicon layers in silicon detector devices," PhD thesis, University of Zagreb, 2017.

[9] E. Gaubas and J. Vanhellemont, "Comparative study of carrier lifetime dependence on dopant concentration in silicon and germanium,"J. Electrochem. Soc., vol. 154, no. 3, pp. H231–H238, 2007.

[10] "Ge - Germanium", Ioffe.ru, 2020. [Online]. Available: http://www.ioffe.ru/SVA/NSM/Semicond/Ge/

[11] E. Gaubas and J. Vanhellemont, "Dependence of carrier lifetime in germanium on resistivity and carrier injection level," Appl. Phys. Lett., vol. 89, no. 14, p. 142106, 2006.

[12] D. Klaassen, "A unified mobility model for device simulation," Int. Tech. Dig. Electron Device, 1990.

[13] S. C. Jain, D. J. Roulston, „A simple expression for band gap narrowing (BGN) in heavily doped Si, Ge, GaAs and GexSi1−x strained layers," Solid-State Electron., vol. 34, no. 5, 1991.

[14] W. C. Dunlap, "Diffusion of impurities in germanium," Phys. Rev., vol. 94, no. 6, pp. 1531–1540, Jun. 1954.

[15] K. Ahlborn, "Diffusion of gallium in germanium along dislocations," J. Phys. Colloq., vol. 40, pp. C6-185., 1979.

[16] U. Södervall et al., "Gallium tracer diffusion and its isotope effect in germanium," Philos. Mag. Lett. A, vol. 54., pp. 539-551., 1986.

[17] I. Riihimäki et al., "Vacancy-impurity complexes and diffusion of Ga and Sn in intrinsic and p-doped germanium," Appl. Phys. Lett., vol. 91, no.9, 2007.

[18] E.N. Sgourou et al., "Diffusion and Dopant Activation in Germanium: Insights from Recent Experimental and Theoretical Results," Appl. Sci., vol.9, no.12, 2019.

[19] M. Werner, H. Mehrer, and H. D. Hochheimer, "Effect of hydrostatic pressure, temperature, and doping on self-diffusion in germanium." Phys. Rev. B, vol. 32, no. 6, 1985.

[20] S. Schneider et al., "Radiation-enhanced self-and boron diffusion in germanium," Phys. Rev. B, vol. 87, no. 11, 2013.

[21] S. M. Hu, "Diffusion in silicon and germanium," in Atomic Diffusion in Semiconductors, D. Shaw, Ed. New York: Plenum, 1973.

[22] S. T. Dunham, and C. D. Wu, "Atomistic models of vacancy-mediated diffusion in silicon," J. Appl. Phys., vol. 78, pp. 2362-2366., 1995.

[23] A. Chroneos, H. Bracht, R. W. Grimes and B.P. Uberuaga, "Vacancy-mediated dopant diffusion activation enthalpies for germanium," Appl. Phys. Lett., vol. 92, no. 17, 2008.

[24] Synopsys, Sentaurus Process User Guide Version P-2019.03. Mountain View, CA, USA: Synopsys, 2019.

[25] S. Uppal, A. F.W.Willoughby, J. M. Bonar, N. E. B. Cowern, T. Grasby, R. J. H. Morris, and M. G. Dowsett, "Diffusion of boron in germanium at 800–900 ◦C," J. Appl. Phys., vol. 96, no. 3, 2004.

[26] S. Uppal et al., "Diffusion of ion-implanted boron in germanium," J. Appl. Phys., vol. 90, no. 8, 2001.

[27] R. W. Olesinski and G. J. Abbaschian, "The Ga–Ge (Gallium-Germanium) system," Bull. Alloy Phase Diagr., vol. 6., no. 3, pp. 258-262, 1985.

[28] L. K. Nanver et al., "Towards CMOS-compatible photon-counting imagers in the whole 10 nm–1600 nm spectral range with PureB Si and PureGaB Ge-on-Si technology," 12th IEEE Int. Conf. Solid-State Integr. Circuit Technol. (ICSICT), 2014

[29] A. Thanailakis, D. Chan and D. Northrop, "Activation energy for the slow states in the aluminium-germanium contact", J. Phys. D: Appl. Phys., vol. 5, no. 10, pp. 1930-1936, 1972.

[30] R. Tung, "The physics and chemistry of the Schottky barrier height", Appl. Phys. Rev., vol. 1, no. 1, p. 011304, 2014.

[31] C. Battaglia, G. Onida, K. Gaál-Nagy and P. Aebi "Structure and stability of the Si (331)–(12×1) surface reconstruction investigated with first-principles density functional theory," Phys. Rev. B, vol 80., no. 21, 2009.